Iranian Journal of Chemical Engineering

Vol. 12, No. 4 (Autumn 2015), IAChE

Effect of graphite oxidation on the yield and quality of graphene synthesized by supercritical exfoliation and its application in photocatalytic degradation of methylene blue

A. Hadi[1], J. Karimi-Sabet[2*], S. M. A. Moosavian[1], S. Ghorbanian[1]

[1]Department of Chemical Engineering, Faculty of Engineering, University of Tehran, Tehran, Iran

[2]NFCRS, Nuclear Science and Technology Research Institute, Tehran, Iran

Abstract

After fullerene and nanotubes, graphene is a new allotrope of carbon. This attractive nanomaterial can be produced by different methods. In this work, we have used the less common approach for preparation of graphene. This technique is based on the utilization of supercritical fluid. Ethanol was used as the solvent for exfoliation of pristine graphite, at the temperature of 400 ^{o}C and pressure of 40 MPa. In addition, supercritical ethanol was used to reduce and exfoliate graphite oxide. FT-IR spectra indicate that reduction and exfoliation of graphite oxide can be done in supercritical ethanol, simultaneously. Effect of graphite oxidation on the yield and quality of graphene was investigated and results showed that oxidation of graphite can improve the yield of supercritical process from 12.5% to 26.8%, but Raman spectra revealed that quality of graphene samples produced by graphite oxide is lower than neat graphite. Moreover, the impacts of initial graphite concentration and sonication power on the exfoliation yield were studied. Finally, hybrid structure of graphene and titanium dioxide nanoparticles were prepared by ultrasonic method and used for photocatalytic degradation of methylene blue dye pollutant. Results revealed that titanium dioxide nanoparticles show better photocatalytic performance in presence of graphene sheets.

Keywords: *Graphene, Graphite, Supercritical Exfoliation, Graphite Oxide, Photocatalytic Degradation*

* Corresponding author: j_karimi@alum.sharif.edu

1. Introduction

Due to its amazing features, graphene became one of the most cited topics of scientific communications in many fields, immediately after its discovery by Geim and Novoselov [1] in 2004. Monolayer graphene with a thickness of only one carbon atom, is the thinnest material known up to now, and at the same time it is the strongest material with Young's modulus of 1 TPa [2]. Other prominent properties of graphene are high thermal conductivity of about 5000 w/m.k [3], excellent electrical conductivity with charge carrier mobility of 2×10^5 $cm^2/V.S$ [4], high theoretical specific surface area of about 2630 m^2/g and superior transmittance of 97.7% to white light for each graphene layer [5]. These features along with the chemical stability and the possibility of being functionalized result in the variety of graphene applications including gas and bio-sensors [6,7], supercapacitors [8], transparent conductive electrodes [9], nanofluids and heat transfer [10-12], polymer nanocomposites [13], catalysis [14], drug delivery [15], gas separation, sorption and storage [16,17], etc.

Different methods have been reported to produce graphene, such as micromechanical cleavage [18], chemical vapor deposition [19], liquid phase exfoliation [20] and chemical approach [21]. All synthesis routes have their advantages and drawbacks, but the main challenge is creating a balance between some parameters to select a proper method. These factors are productivity, process costs, environmental issues and the quality of produced graphene.

Among all these methods, chemical exfoliation is the most common and promising technique to produce graphene in a large scale. This approach consists of oxidation and exfoliation of graphite to graphene oxide followed by its reduction. In this case, the major drawback is the high toxicity of reductive reagents such as hydrazine and its derivatives, thus some studies have been performed to introduce green reductive agents like vitamin C [22], amino acids [23] and phytochemicals [24]. In this regard, some researches were done about the reduction of graphene oxide in supercritical fluids like CO_2 and alcohols [25,26]. Generally, supercritical fluids are known as green solvents for different kinds of processes such as chromatography [27], solid and liquid extraction [28], chemical and enzymatic reactions [29,30], polymer processing [31], drying [32], electrochemistry [33] and so on. Supercritical fluids with low calcination temperature are useful to reduce graphene oxide [25]. Furthermore, other properties of supercritical fluids such as high diffusivity, low viscosity and zero surface tension make them good solvents for exfoliation of pristine graphite to graphene without any oxidation process. This technique is based on diffusion of supercritical fluid molecules into the space between graphite layers and its expansion, and was reported by some groups in literature [34-36].

In this study, both graphite and graphite oxide were successfully used to synthesize graphene by supercritical fluid exfoliation in ethanol. The effect of oxidation on the yield and quality of graphene sheets was investigated and the products were

characterized. Besides, the influence of graphite concentration and sonication power on the exfoliation yield was obtained. Finally, the prepared graphene sheets were utilized to improve the catalytic performance of TiO_2 nanoparticles in degradation of methylene blue under UV light irradiation.

2. Experimental section

2-1. Materials

Graphite powder with particle size less than 50 μm, ethanol (99.8% purity), sulfuric acid, potassium permanganate ($KMnO_4$), sodium nitrate ($NaNO_3$), hydrogen peroxide (30%) and methylene blue (MB) were purchased from Merck Co. Titanium dioxide (TiO_2) nanoparticles (P25–DEGUSSA, particle size=21 nm) was supplied by Sigma-Aldrich.

2-2. Methods

2-2-1. Preparation of graphite oxide (GO)

Graphite oxide powder was prepared by well-known Hummers method involving graphite treatment using H_2SO_4, $KMnO_4$, $NaNO_3$ and H_2O_2. Detailed procedure can be obtained from the reference [37].

2-2-2. Supercritical exfoliation process

In a typical experiment, first dispersion of graphite or graphite oxide with a concentration of 0.25 mg/mL was prepared in ethanol, by sonication for 15 min. Then, the suspension was transferred to a 170 mL stainless steel reactor and heated up to 400^{o}C, while the pressure of 40 MPa was adjusted by the ethanol volume. The reactor was cooled in an ice-water bath, after one hour. The dispersion was centrifuged to remove the unchanged graphite particles. Finally the product was filtered and dried at 60^{o}C overnight. Moreover, the yield of graphene synthesis was determined by dividing the graphene concentration by the initial graphite concentration, while the concentration of exfoliated graphene in final suspension can be obtained by measuring the absorbance of graphene at 660 nm and using Beer – Lambert law (Eq. 1).

$$\frac{A}{l} = \alpha\, c \qquad (1)$$

where c (mg/mL) is the graphene concentration in the suspension, A/l (1/m) is the absorbance per cell length and α (mg/mL.m) is the absorption coefficient. The experimentally calculated α was about 273.2 mg/mL.m.

2-2-3. TiO_2–graphene composite

Hybrid structure of graphene sheets and TiO_2 nanoparticles was prepared by simple solution mixing method [38,39]. Briefly, Graphene sheets (derived from supercritical conversion of GO) and TiO_2 nanoparticles with mass ratio of 1:3 were mixed in ethanol, under high power sonication for one hour. The products were collected via centrifugation of final suspension and dried.

2-2-4. Photocatalytic experiments

In a de-colorization experiment, 100 mL aqueous solution of methylene blue was prepared in which the initial concentration of dye was 5 mg/L. Then, 100 mg of photocatalyst (pure TiO_2 or TiO_2-RGO) was added to the solution. A homogenous

suspension was obtained by high power sonication. The suspension was stirred in the dark for about 30 min which is enough to reach the adsorption/desorption equilibrium [40] and no significant changes were observed in MB concentration. After that, the resulting aqueous suspension was put into the photo-reactor and subjected to UV light irradiation. The photo-reactor system is a cubic aluminum vessel involving three UV lamps (UVC, 6 W, CH lighting, China) with wavelength of 253 nm as a catalyst excitation source, a magnetic stirrer to make uniform mixture during UV irradiation, and a circulator to keep the solution temperature at 25°C during the process. During the experiment, 10 mL of the solution was decanted through certain time intervals, and centrifuged (9000 rpm, 20 min) to remove the suspended catalyst. Finally, the concentration of MB was determined by measuring the optical absorbance of supernatant at 660 nm, and at different irradiation times.

2-3. Characterization

Optical absorbance measurements were performed by UV-vis spectrometer (Mecasys, OPTIZEN POP, Korea). SEM analysis was performed using a scanning electron microscope (Seron Technology, AIS2100, Korea). FT-IR spectra were recorded using a Bruker Vector 22 spectrometer with KBr as a background. TEM images were taken by transmission electron microscope (Zeiss-EM10C-80 KV, Germany). AFM imaging was carried out by means of an atomic force microscope (Park scientific Instruments CP-Research (VEECO), USA) on the tapping mode. X-ray diffraction (XRD) patterns were obtained using an X-ray diffractometer (STOE, STIDY-MP, Germany). Raman spectra were recorded using Raman spectrometer (Horiba Jobin Yvon, LabRAM HR 800) with excitation wavelength of 532 nm.

3. Results and discussion

Fig. 1 shows SEM image of initial graphite powder. Ultra-thin graphene sheets can be obtained by supercritical exfoliation technique. Thanks to the special features of supercritical fluids that are the combination of liquid and gas states including transport properties and high solvent strength, ethanol molecules at supercritical condition can easily diffuse and intercalate between graphitic layers which weaken interlayer forces. Then, thermal stresses due to the rapid cooling at the end of process, along with the transition from the supercritical state to liquid phase can implement the exfoliation.

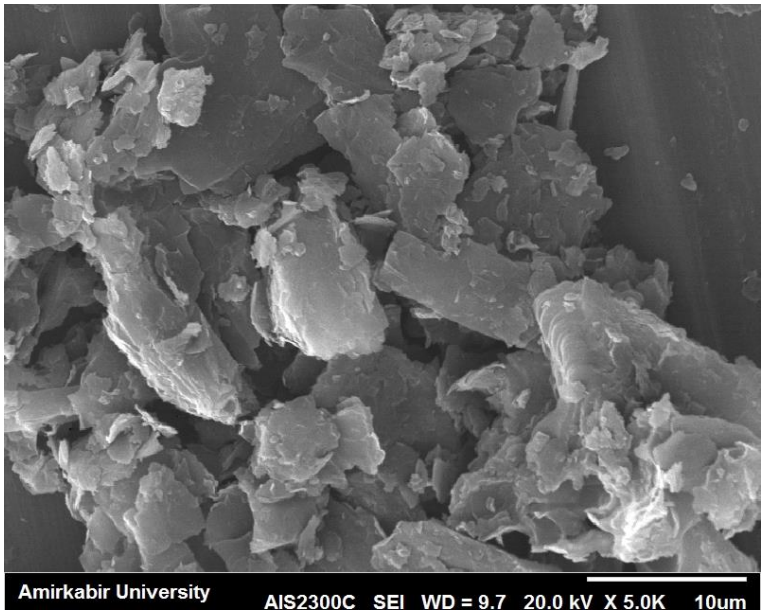

Figure 1. SEM image of graphite flakes deposited on the surface of aluminum foil substrate.

TEM images of graphene sheet exfoliated in supercritical ethanol are shown in Fig. 2. It is evident that the relative transparency is due to the conversion of graphite to few layer graphene.

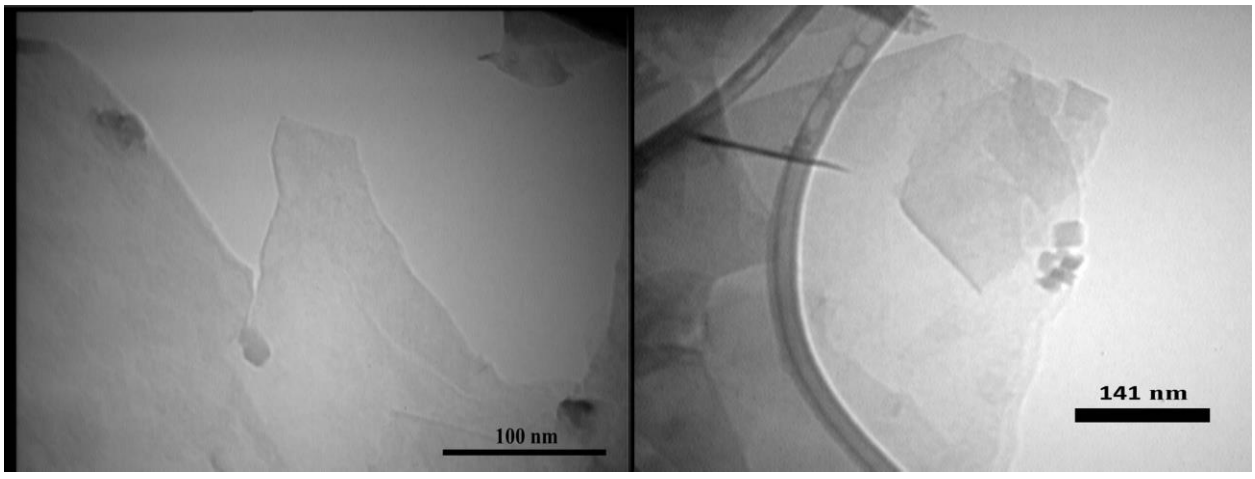

Figure 2. TEM images of graphene sheets obtained from exfoliation of neat graphite in supercritical ethanol.

Fig. 3 illustrates AFM image of graphene sheets deposited on the clean surface of mica substrate. The thickness of about 0.78 nm and 2 nm ensured the exfoliation of graphite to single and few-layer graphene.

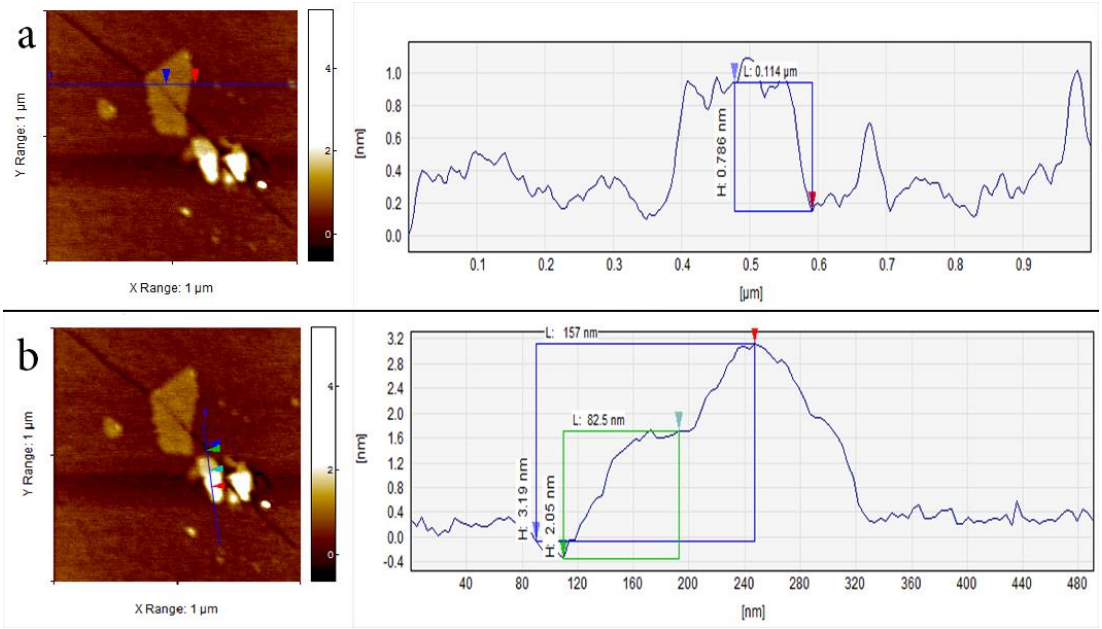

Figure 3. AFM images of exfoliated graphene sheets.

3-1. Process variables

3-1-1. Effect of graphite concentration

The effect of graphite concentration on the exfoliation yield was investigated in the range of 0.25–1 mg/mL (Fig. 4). It can be seen that by increasing graphite concentration, the yield of process decreases. It is related to the number of ethanol molecules that intercalates between layers which are lower at the higher concentrations. Furthermore, the higher amount of dispersed graphite flakes results in the greater contact between immersed graphene sheets and further aggregation the more aggregation of exfoliated sheets.

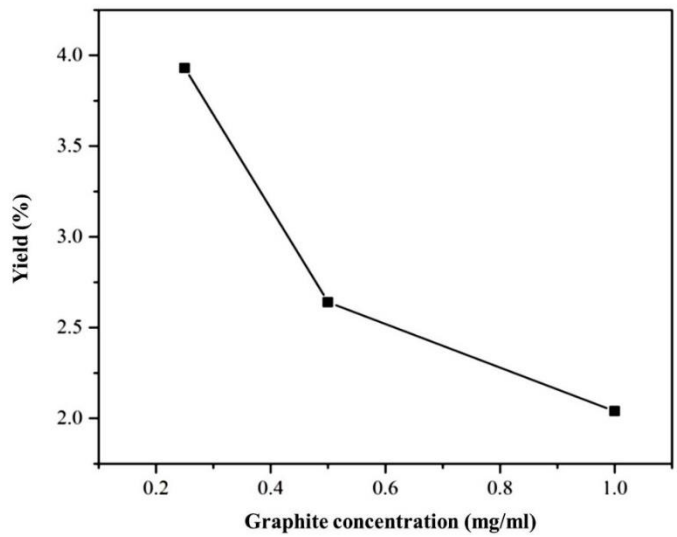

Figure 4. Effect of graphite concentration on the yield of supercritical exfoliation process at reduced temperature and pressure of T_r, P_r=1.1.

3-1-2. Effect of sonication power

Fig. 5 represents the effect of sonication power (before supercritical treatment) on the yield of exfoliation. The sonication power was varied in the range of 80–160 W and the results show the positive influence of this parameter on the yield. By increasing the sonication power, graphite flakes receive more energy through sonication that results in the better stability of graphite dispersion during the process which improves the yield.

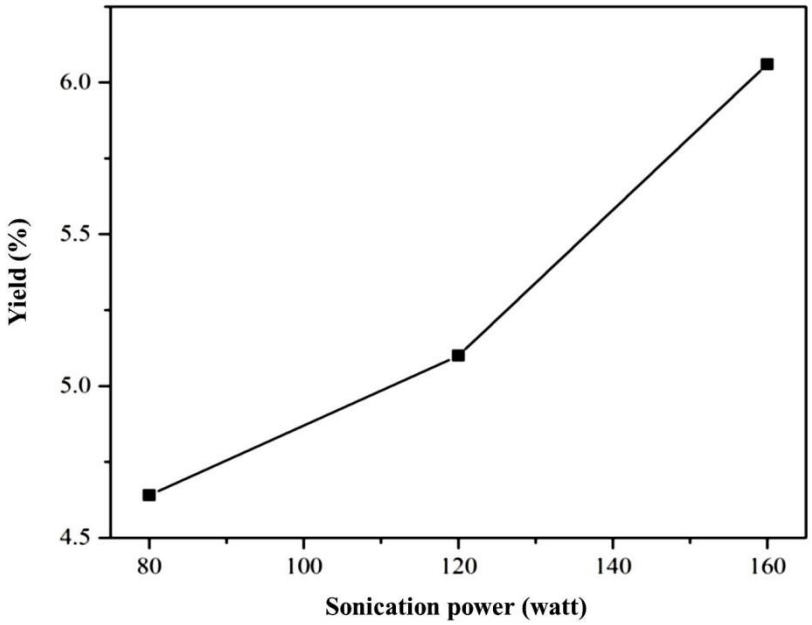

Figure 5. Effect of sonication power on the yield of supercritical exfoliation process at reduced temperature and pressure of T_r, P_r=1.1.

3-1-3. Effect of graphite oxidation

Graphite and GO were used in supercritical ethanol process at temperature of 400°C and pressure of 40 MPa to investigate the impact of graphite oxidation. It must be stated that initial concentration of precursors and the sonication power were fixed at 0.25 mg/mL and 120 W. Graphene sheets that were produced by graphite and graphite oxide (GO) are denoted by "GS" and "RGO", respectively.

In the case of GO precursor, first it should be demonstrated that reduction can be carried out along with the exfoliation. UV-vis spectra of RGO sample and digital photographs of GO and RGO dispersions are shown in Fig. 6. The color change of dispersion from brown to black after supercritical process is a visual characteristic of GO reduction, which can be clearly seen in Fig. 6 (inset).

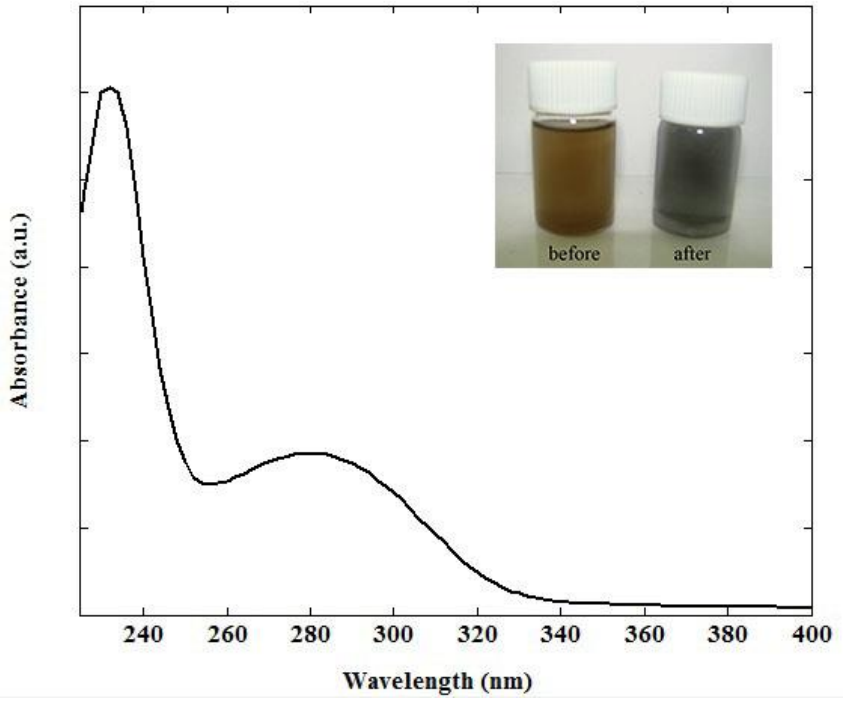

Figure 6. UV-vis spectra of RGO, inset) color change of graphite oxide (GO) after treatment in supercritical ethanol.

Also, FT-IR spectra was used to confirm the reduction of GO under supercritical ethanol condition. All vibrational modes of different oxygen functional groups in the FTIR spectra of GO comprise: C-O-C (1230-1320 cm^{-1}), C=C (1500-1600 cm^{-1}), COOH (1650-1750 cm^{-1}), C=O (1600-1650, 1750-1850 cm^{-1}) and C-OH (3050-3800 cm^{-1}) [41]. Comparison of two spectra before and after the supercritical treatment in Fig. 7 shows that a degree of reduction occurred by supercritical process. This is due to the coupled effects of thermal reduction by high temperature and chemical reduction through the reductive character of supercritical alcohols owing to their hydrogen donation, which leads to the removal of oxygen functional groups from GO structure [26].

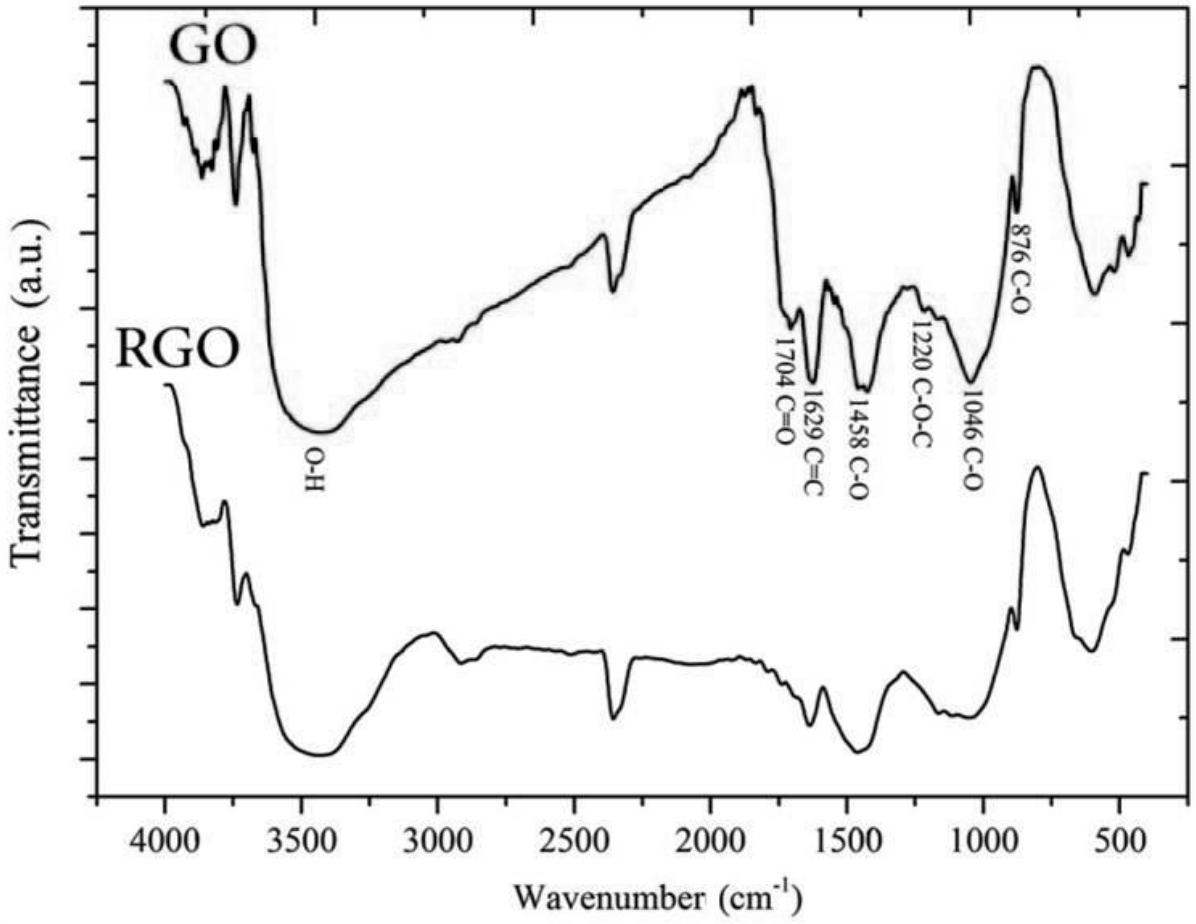

Figure 7. FT-IR spectra of graphite oxide (GO) and RGO samples.

Fig. 8a represents TEM images of RGO samples. The morphologies of graphene sheets prepared from graphite and GO have an obvious difference. In comparison to graphene sheets that are prepared from pristine graphite (Fig. 2), RGO sheets have a more wrinkled structure that can be seen in Fig. 8a. The wrinkled morphology of RGOs may be related to the oxidation and reduction steps.

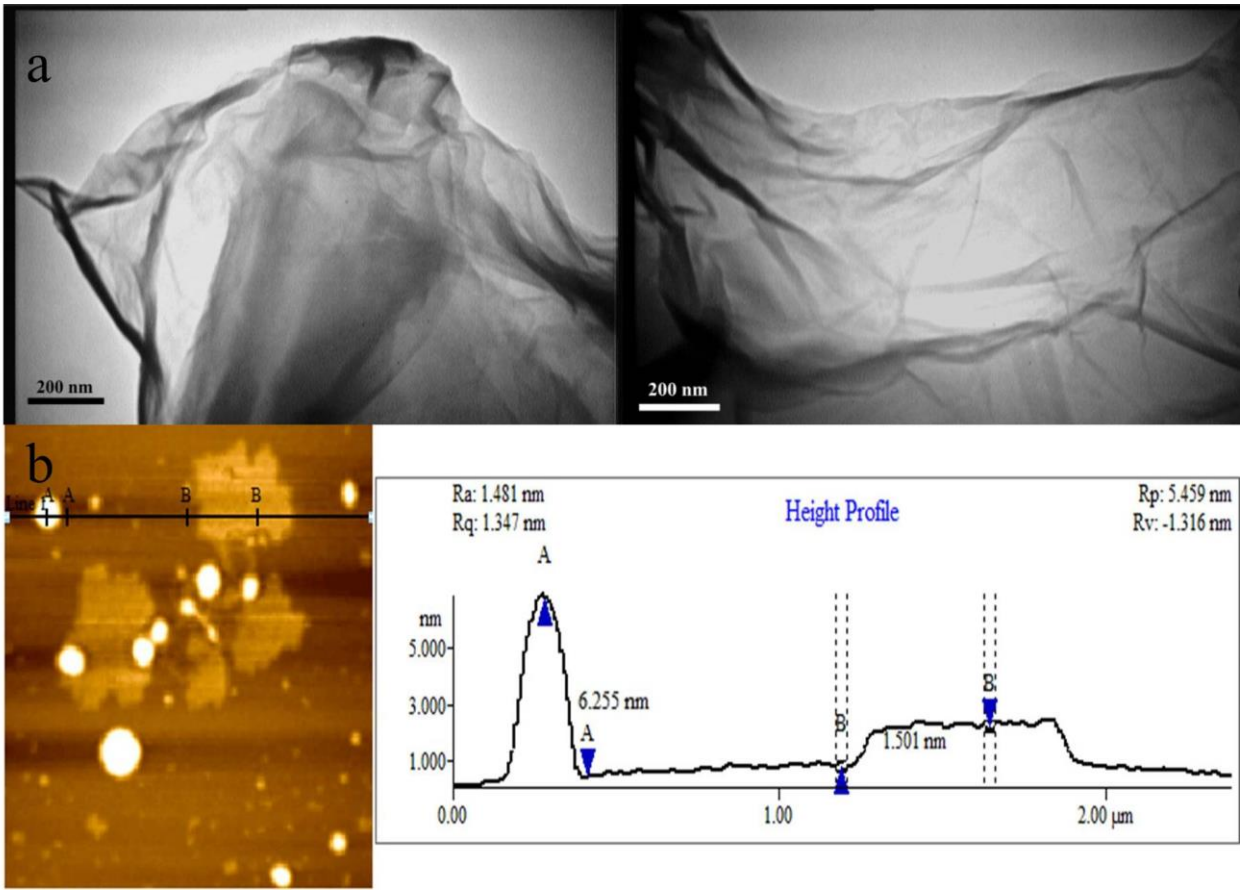

Figure 8. a) TEM images of graphene sheets obtained from exfoliation of graphite oxide (GO) in supercritical ethanol. b) AFM image of RGO sample along with the height profile.

A typical AFM image of RGO sample is shown in Fig. 8b. The sheet with the thickness of about 1.5 nm can be observed which corresponds to 1-3 layers of graphene. Furthermore, some particles with the larger thickness (6.2 nm) were detected in this figure that may be due to the aggregation of sheets during reduction.

Generally, oxidation of graphite leads to the introduction of oxygen functionalities including hydroxyl, epoxy, carbonyl and carboxyl groups into its structure which increases the interlayer distances. This can be seen at XRD patterns which, after oxidation, diffraction peak of graphite shifts to lower angle (Fig.9a). By means of XRD pattern and using Bragg equation, the interlayer distance for graphite and GO were obtained 3.36Å and 7.37Å, respectively. This expansion in the interlayer space of graphite after its oxidation can reduce van der Waals interactions between the layers. In addition, this expansion provides more space for diffusion of supercritical fluid molecules and enhances the exfoliation rate, which increases the yield of graphene synthesis from 12.5% to 26.8% for graphite and GO, respectively.

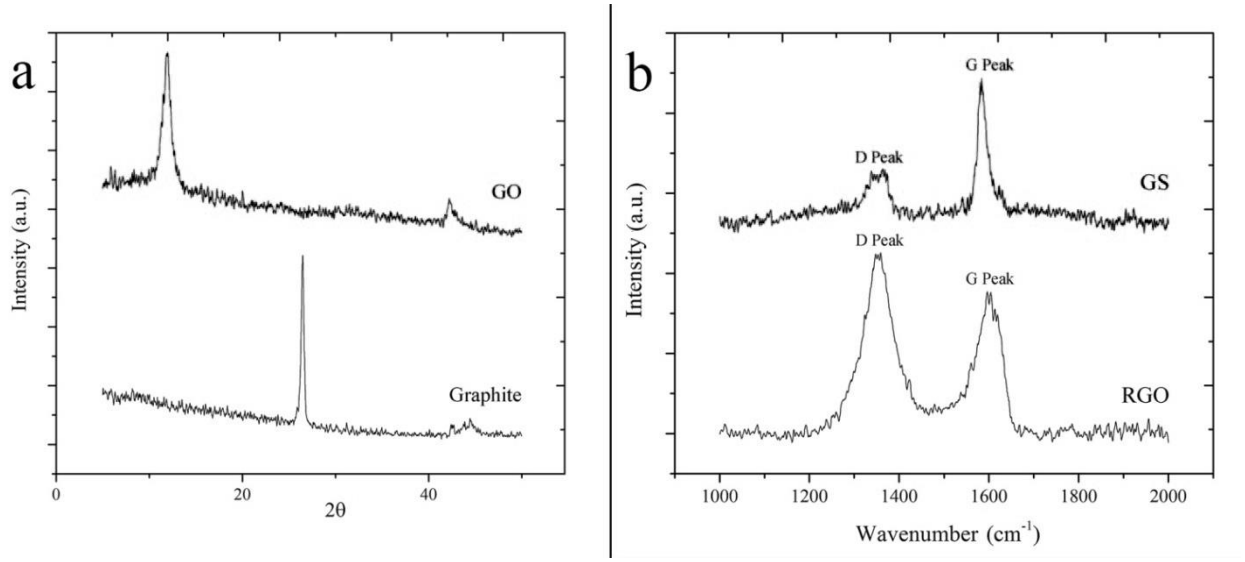

Figure 9. a) XRD patterns of pristine graphite and graphite oxide (GO) and b) Raman spectra of graphene samples derived from graphite (GS) and graphite oxide (RGO).

Raman spectroscopy was used to investigate the quality of graphene sheets. In the Raman spectra of graphene, D peak (around 1350 cm^{-1}) arises from structural defects in sample and the intensity ratio of D to G peak is utilized to evaluate the amount of graphene defects. Fig. 9b shows Raman spectra of graphene produced by both precursors. The intensity ratio of I_D/I_G in RGO and GS samples are 1.28 and 0.36. This shows that oxidation of graphite considerably reduces the product quality which relates to the residual oxygen functionalities that cannot be eliminated completely from GO structure through supercritical process, similar to any reduction approach. Fig. 10 shows the schematic diagram of graphene preparation by supercritical exfoliation of graphite and GO.

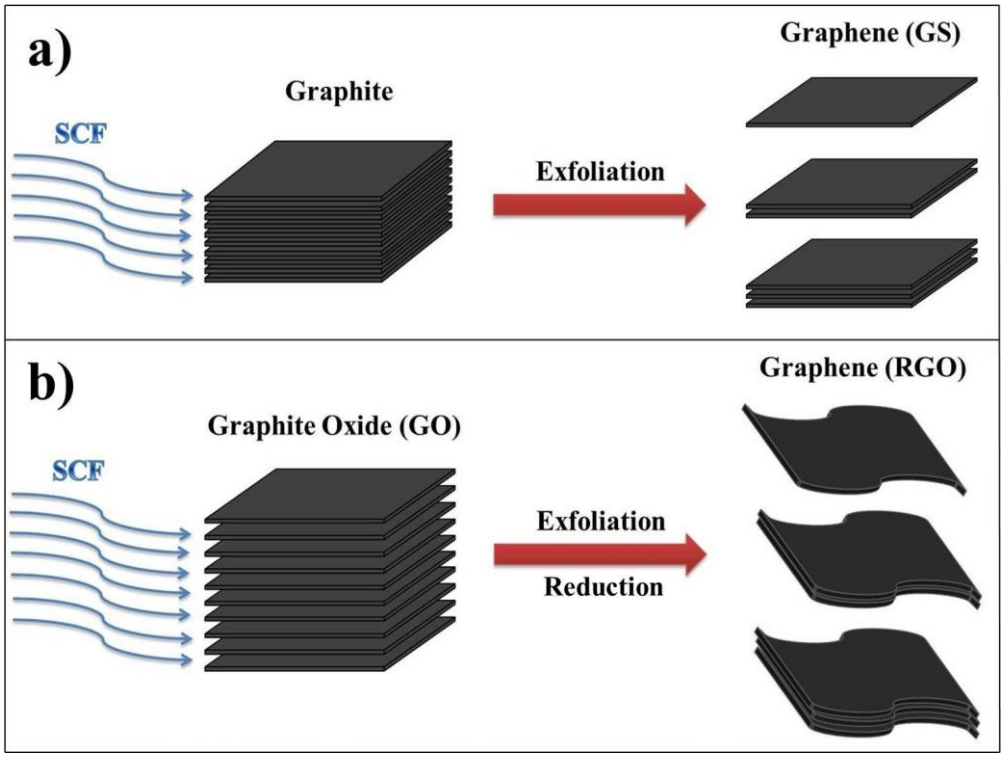

Figure 10. Schematic image showing the supercritical fluid (SCF) exfoliation of a) graphite and b) graphite oxide (GO) to graphene.

3-2. Phtocatalytic performance of graphene–TiO_2 hybrid

Organic dyes are one of the most important sources of water pollution. Dyeing and textile industries introduce a large volume of wastewater into the environment that contains a considerable amount of organic dyes. The presence of these dyes in the water threatens the aquatic life by eutrophication, disturbing the photosynthetic activity and introducing the toxic compounds like aromatics and chlorides [42]. Being aware of the serious environmental impacts of dye pollutants is the motivation to probe new approaches or developing the available methods for wastewater purification. As the organic dyes show resistance against biological degradation, the advanced oxidation processes (AOP) such as photocatalysis are developed for the removal of these pollutants. Methylene blue (MB) is an aromatic and cationic azo-dye that has wide applications, especially in textile industry. The photocatalytic oxidation over metal oxide nanoparticles such as TiO_2, ZnO and Fe_2O_3 is a common method for degradation of MB. The oxidative decomposition mechanism of methylene blue under UV irradiation has been investigated in detail elsewhere [43]. On the other hand, the application of graphene based photocatalyts in degradation of pollutants is a growing field [44]. Herein, we produced the graphene/TiO_2 hybrid structure (TiO_2-RGO) to use as photocatalyst for degradation of methylene blue.

Fig. 11 shows the TEM images of as-prepared TiO_2-RGO structure. It can be seen that TiO_2 nanoparticles are well deposited on

the surface of graphene sheets. This may relate to wrinkled morphology of RGO that provides the opportunity for uniform deposition of nanoparticles on the surface of RGO sheets. Furthermore, the residual oxygen functionalities on the RGO structure can act as sites for adsorption of TiO_2 nanoparticles.

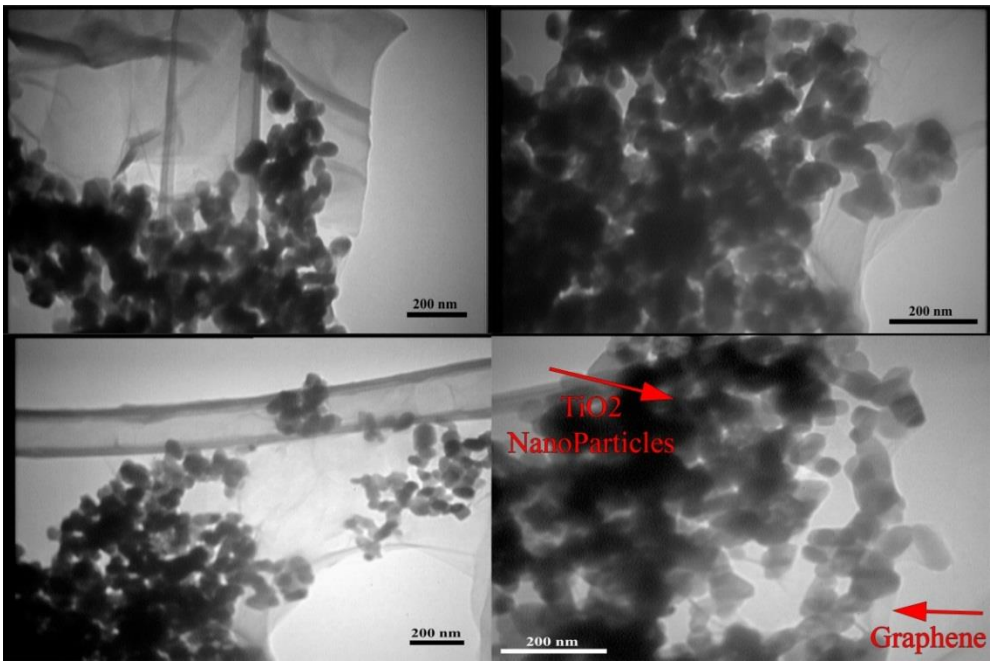

Figure 11. TEM images of TiO_2-RGO sample.

After performing the photocatalytic experiments under UV irradiation and using two types of photocatalysts (TiO_2, TiO_2-RGO), the changes in the concentration of methylene blue with irradiation time was obtained which is shown in Fig. 12a. It could be seen that at the same irradiation times, the concentration of MB over TiO_2-RGO photocatalyst is lower than pure TiO_2, which shows that the TiO_2-RGO has a better efficiency in degradation of methylene blue.

The decomposition reaction of MB under UV irradiation has been considered as a pseudo first order model as the following equation [43]:

$$r = k\,c \tag{2}$$

where r is the reaction rate, k is apparent rate constant and c denotes the concentration of MB in the aqueous solution. In order to ascertain the photocatalytic activity of TiO_2 and TiO_2–RGO samples, the rate constants should be calculated using Eq. 3.

$$\ln\left(\frac{c_0}{c}\right) = kt \tag{3}$$

In this equation, c_0 represents the initial concentration of MB and t is the irradiation time. Thus, $ln(^{c_0}/_{c})$ was plotted against the irradiation time (t) to obtain the reaction rate constant (k) which is the slope of fitted lines (Fig. 12b).

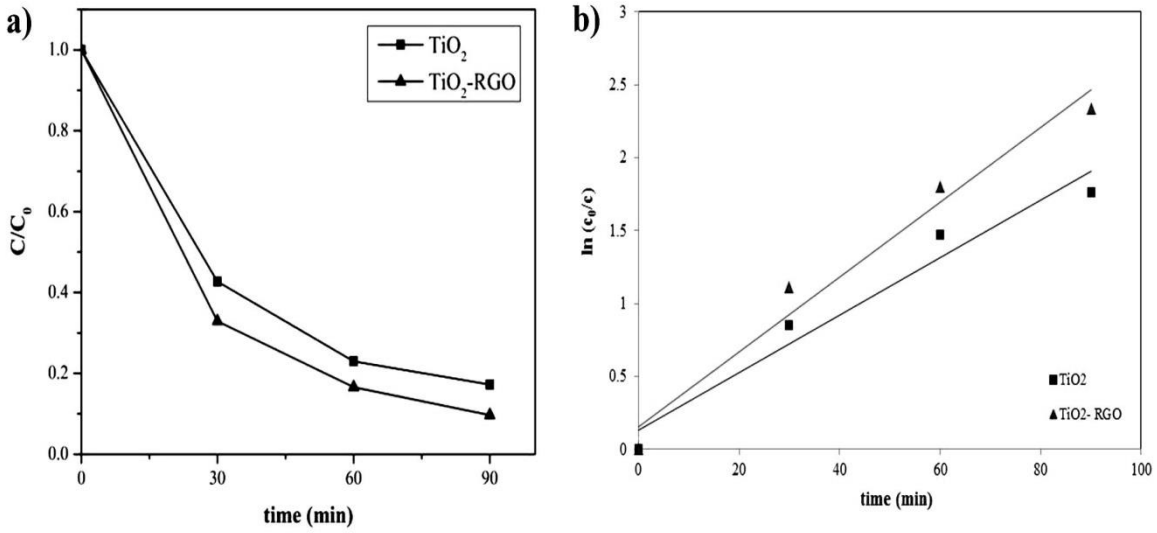

Figure 12. Photocatalytic degradation of methylene blue (MB) under UV light irradiation and over pure TiO_2 and prepared RGO-TiO_2 phtocatalysts: a) normalized concentration of MB versus irradiation time and b) logarithm scale of (a) to obtain the rate constants.

The values of 0.95 and 0.97 for the regression coefficient (R^2) of TiO_2 and TiO_2 – RGO samples show that these experimental data are well fitted on the straight lines which confirms the first order kinetic for degradation of MB under UV irradiation. The calculated rate constant for TiO_2 and TiO_2 – RGO are 1.97×10^{-2} and 2.57×10^{-2} min^{-1}, respectively. This result proves that the presence of graphene sheets results in the higher activity of TiO_2 nanoparticles in this photocatalytic process. This enhancement is due to the excellent charge transfer of graphene that prevents the well-known problem in photocatalytic processes which is the electron – hole recombination.

4. Conclusions

From different aspects, the supercritical exfoliation is a unique method for graphene production. This is a fast and green approach and uses inexpensive source of graphite. Moreover, supercritical exfoliation has an acceptable yield that allows it to be scaled up and turned into the reliable option for graphene based applications. Results showed that oxidation of graphite improves the yield of graphene production, but product quality is not as good as pristine graphite. Depending on whether quality or quantity is needed in the specified application, both precursors can be used in this process. The prepared graphene sheets were combined with TiO_2 nanoparticles and used to remove methylene blue from aqueous solution using UV irradiation. Results revealed that calculated rate constant for degradation reaction of methylene blue over graphene – titanium dioxide photocatalyst is about 30% more than pure titanium dioxide.

References

[1] Novoselov, K. S. Geim, A. K. Morozov, S. V. Jiang, D. Zhang, Y. Dubonos, S. V. Grigorieva, I. V. and Firsov A. A., "Electric field effect in atomically thin carbon films", *Sci*., **306** 666 (2004).

[2] Lee, C. Wei, X. Kysar, J. W. and Hone, J., "Measurement of the elastic properties and intrinsic strength of monolayer graphene", *Sci*., **321** (5887), 385 (2008).

[3] Balandin, A. A. Ghosh, S. Bao, W. Teweldebrhan, I. D. Miao, F. and Lau, C. N., "Superior thermal conductivity of single-layer graphene", *Nano Lett*., **8** (3), 902 (2008).

[4] Bolotin, K. I. Sikes, K. J. Jiang, Z. Klima, M. Fudenberg, G. Hone, J. Kim, P. and Stormer H. L., "Ultrahigh electron mobility in suspended graphene", *Solid State Commu.*, **146** (9-10), 351 (2008).

[5] Nair, R. R. P. Blake, A. N. Grigorenko, K. S. Novoselov, T. J. Booth, T. Stauber, N. Peres, M. R. and Geim, A. K., "Fine structure constant defines visual transparency of graphene", *Sci.*, **320**, 1308 (2008).

[6] Basu, S. and Bhattacharyya, P., "Recent developments on graphene and graphene oxide based solid state gas sensors", *Sens. Actuators B: Chem.*, **173**, 1 (2012).

[7] Kuila, T. Bose, S. Khanra, P. Mishra, A. K. Kim, N. H. and Lee, J. H., "Recent advances in graphene-based biosensors", *Biosens. Bioelectron.*, **26** (12), 4637 (2011).

[8] Stoller, M. D. Park, S. Zhu, Y. An, J. and Ruoff, R. S., "Graphene-based ultracapacitors", *Nano Lette.*, **8** (10), 3498 (2008).

[9] Wang, L., "Graphene-based transparent conductive electrodes for GaN-based light emitting diodes: Challenges and countermeasures", *Nano Energy*, **12**, 419 (2015).

[10] Yu, W. Xie, H. and Wang, X., "Significant thermal conductivity enhancement for nanofluids containing graphene nanosheets", *Phy. Lett. A*, **375** (10), 1323 (2011).

[11] Kole M. and Dey, T. K., "Investigation of thermal conductivity, viscosity, and electrical conductivity of graphene based nanofluids", *J. Appl. Phys.*, **113** (8), (2013).

[12] Baby T. T. and Ramaprabhu, S., "Enhanced convective heat transfer using graphene dispersed nanofluids", *Nanoscale Res. Lett.*, **6** (1), 289 (2011).

[13] Hu, K. Kulkarni, D. D. Choi, I. and Tsukruk, V. V., "Graphene-polymer nanocomposites for structural and functional applications", *Prog. Polym. Sci.*, **39** (11), 1934 (2014).

[14] Hu, H. Xin, J. H. Hu, H. Wang, X. and Kong, Y., "Metal-free graphene-based catalyst—Insight into the catalytic activity: A short review", *App. Catal. A: General*, **492**, 1 (2015).

[15] S. Goenka, V. Santa, and S. Sant, "Graphene-based nanomaterials for drug delivery and tissue engineering", *J. Controlled Release*, **173**, 75 (2014).

[16] S. Gadipelli and Z.X. Guo, "Graphene-based materials: Synthesis and gas sorption, storage and separation", *Prog. Mater. Sci.*, **69**, 1 (2015).

[17] Hauser, A. W. Schrier, J. and Schwerdtfeger, P., "Helium tunneling through nitrogen-functionalized graphene pores: pressure- and temperature-driven approaches to isotope separation", *J. Phys. Chem.*, **116** (19), 10819 (2012).

[18] Novoselov, K. Jiang, S. Schedin, D. F. Booth, T. J. Khotkevich,V. V. Morozov, S. V. and Geim, A. K., "Two-dimensional atomic crystals", *PNAS*, **102** (30), 10451 (2005).

[19] Liu, W. Li, Xu, H. Khatami, C. Y. and Banerjee, K., "Synthesis of high-quality monolayer and bilayer graphene on copper using chemical vapor deposition", *Carbon*, **49** (13), 4122 (2011).

[20] Hernandez, Y., "High-yield production of graphene by liquid-phase exfoliation of graphite", *Nat. Nanotech.* **3**, 563 (2008).

[21] Stankovich, S. Dikin, D. A. Piner, R. D. Kohlhaas, K. A. Kleinhammes, A. Jia, Y. Wu, Y. Nguyen, S. T. and Ruoff, R. S., "Synthesis of graphene-based nanosheets via chemical reduction of exfoliated graphite oxide", *Carbon*, **45** (7), 1558 (2007).

[22] Gao, J. Liu, F. Liu, Y. Ma, N. Wang, Z. and Zhang, X., "Environment-Friendly Method To Produce Graphene That Employs Vitamin C and Amino Acid", *Chem. Mat.*, **22** (7), 2213 (2010).

[23] Tran, D. N. H. Kabiri, S. and Losic, D., "A green approach for the reduction of graphene oxide nanosheets using non-aromatic amino acids", *Carbon*, **76**, 193 (2014).

[24] Thakur, S. and Karak, N., "Green reduction of graphene oxide by aqueous phytoextracts", *Carbon*, **50** (14), 5331 (2012).

[25] Kong, C. Y. Song, W. L. M. Meziani, Tackett, J. K. Cao, N. L. Farr, A. J. Anderson, A. and Sun,Y. P., "Supercritical fluid conversion of graphene oxides", *J. Supercrit. Fluids*, **61** 206 (2012).

[26] Seo, M. Yoon, D. Hwang, K. S. Kang, J. W. and Kim, J., "Supercritical alcohols as solvents and reducing agents for the synthesis of reduced graphene oxide", *Carbon*, **64**, 207 (2013).

[27] Kalikova, K. Slechtova, T. Vozka, J. and Tesarova, E., "Supercritical fluid chromatography as a tool for enantioselective separation; A review", *Anal. Chim. Acta*, **821**, 1 (2014).

[28] Knez, Z. Skerget, M. and Hrncic, M. K., Principles of supercritical fluid extraction and applications in the food, beverage and nutraceutical industries, in: S. S. H. Rizvi (Eds.), Separation, extraction and concentration processes in the food, beverage and nutraceutical industries, Woodhead Publishing, Great Abington, p. 3 (2013).

[29] Knez, Z., "Enzymatic reactions in dense gases", *J. Supercrit. Fluids*, **47** (3), 357 (2009).

[30] Jessop, P. G. and Leitner, W. Supercritical fluids as media for chemical reactions, in: P. G. Jessop and W. Leitner (Eds.), Chemical Synthesis Using Supercritical Fluids, Wiley-VCH Verlag GmbH, Weinheim, p. 1 (1999).

[31] Higginbotham, C. L. J. Yons, G. L. and Kennedy, J. E., Polymer processing using supercritical fluids, in: S. Thomas and Y. Weimin (Eds.), Advances in polymer processing from macro to nano scale, Woodhead Publishing, Great Abington, p. 384 (2009).

[32] Brown, Z. K. Fryer, P. J. Norton, I. T. and Bridson, R. H., "Drying of agar gels using supercritical carbon dioxide", *J. Supercrit. Fluids*, **54** (1), 89 (2010).

[33] Toghill, K. E. Méndez, M. A. and Voyame, P., "Electrochemistry in supercritical fluids: A mini review", *Electrochem. Commun.*, **44**, 27 (2014).

[34] Rangappa, D. Sone, K. Wang, M. Gautam, U. K. Golberg, D. Itoh, H. Ichihara, M. and Honma, I., "Rapid and direct conversion of graphite crystals into high-yielding, good-quality graphene by supercritical fluid exfoliation", *Chem. Eur. J.*, **16** 6488 (2010).

[35] Liu, C. Hu, G. and Gao, H., "Preparation of few-layer and single-layer graphene by exfoliation of expandable graphite in supercritical N,N-dimethylformamide", *J. Supercrit. Fluids*, **63** 99 (2012).

[36] Pu, N. W. Wang, C. A. Sung, Y. Y. Liu, M. and Ger, M. D., "Production of few-layer graphene by supercritical CO2 exfoliation of graphite", *Mat. Lett.*, **63** (23), (2009).

[37] Marcano, D. C. Kosynkin, D. V. Berlin, J. M. Z. Sinitskii, S. A. Slesarev, A. L. Alemany, B. Lu, W. and Tour, J. M., Tour, "Improved synthesis of graphene oxide", *ACS Nano*, **4** (8), 4806 (2010).

[38] Meidan, Y. Miaoqiang, L. Chang, C. James, I. Changjian, L. and Zhiqun, L. Design, fabrication and modification of cost-effective nanostructured TiO2 for solar energy applications, in: W. Jun and L. Zhiqun (Eds.), Low-Cost Nanomaterials, Springer, London, p. 41 (2014).

[39] Zhang, X. and Cui, X., Graphene/Semiconductor Nanocomposites: Preparation and Application for Photocatalytic Hydrogen Evolution, in: F. Ebrahimi (Eds.), Nanocomposites - New Trends and Developments, InTech, Rijeka, Croatia, p. 243 (2012).

[40] Xu, C. G. Rangaiah, P. and Zhao, X. S., "Photocatalytic degradation of methylene blue by titanium dioxide: experimental and modeling study", *Ind. Eng. Chem. Res.*, **53** (38), 14641 (2014).

[41] Acik, M. Lee, G. Mattevi, C. Chhowalla, M. Cho, K. and Chabal, Y. J. "Unusual infrared-absorption mechanism in thermally reduced graphene oxide", *Nat. Mat.*, **9**, 840 (2010).

[42] Zollinger, H., Color Chemistry: Syntheses, Properties, and Applications of Organic Dyes and Pigments, VCH, New York, p. 92 (1987).

[43] Houas, A. Lachheb, H. Ksibi, M. Elaloui, Guillard, E. C. and Herrmann, J. M., "Photocatalytic degradation pathway of methylene blue in water", *Appl. Catal. B: Environ.* **31** (2), 145 (2001).

[44] Zhang, N. Y. and Xu, Y. J., "Recent progress on graphene-based photocatalysts: current status and future perspectives", *Nanoscale*, **4** (19), 5792 (2012).